Trimodal spectroscopy for the detection and characterization of cervical precancers in vivo

Irene Georgakoudi, PhD,[a] Ellen E. Sheets, MD,[b] Markus G. Müller, MSc,[a] Vadim Backman, PhD,[a] Christopher P. Crum, MD,[c] Kamran Badizadegan, MD,[d] Ramachandra R. Dasari, PhD,[a] and Michael S. Feld, PhD[a]

Cambridge and Boston, Mass

OBJECTIVE: The objective of this study was to assess the potential of 3 spectroscopic techniques (intrinsic fluorescence, diffuse reflectance, and light scattering) individually and in combination (trimodal spectroscopy) for the detection of cervical squamous intraepithelial lesions.

STUDY DESIGN: The study was conducted with 44 patients who underwent colposcopy for the evaluation of an abnormal Papanicolaou smear. Fluorescence and reflectance spectra were collected from colposcopically normal and abnormal sites and analyzed to extract quantitative information about tissue biochemistry and morphologic condition. This information was compared with histopathologic classification, and diagnostic algorithms were developed and validated with the use of logistic regression and cross-validation.

RESULTS: Diagnostically significant differences exist in the composition of fluorescing biochemicals, the scattering properties, and the epithelial cell nuclear morphology of cervical squamous intraepithelial lesions and non–squamous intraepithelial lesions. Trimodal spectroscopy is a superior tool for the detection of cervical squamous intraepithelial lesions than any 1 of the techniques alone.

CONCLUSION: Trimodal spectroscopy has the potential to improve the in vivo detection of precancerous cervical changes. (Am J Obstet Gynecol 2002;186:374-82.)

Key words: Cancer, diagnostic, spectroscopy, fluorescence, diffuse reflectance, light scattering, cervical neoplasia

Spectroscopic techniques examine the interactions of light with biologic tissue and provide information about the biochemical and structural tissue composition. Techniques that use near-UV and visible light are easily implemented in vivo in a clinical setting and can provide feedback with respect to the properties that they assay in real time. Thus, they could serve as a useful guide in the detection of biochemical and/or morphologic changes that reflect the presence of precancerous and early cancerous lesions. In addition, the capability to monitor such changes in vivo could enhance our understanding of some of the fundamental events that are involved in neoplastic progression.

From the G.R. Harrison Spectroscopy Laboratory, Massachusetts Institute of Technology[a]; the Department of Obstetrics and Gynecology, Division of Gynecologic Oncology,[b] and the Department of Pathology, Division of Women's and Perinatal Pathology,[c] Brigham & Women's Hospital; and the Department of Pathology, Children's Hospital.[d]

Supported in part by National Institutes of Health National Research Service Award grant F32CA80345 (I.G.) and by NIH grant P41RR02594.

Received for publication April 4, 2001; revised July 27, 2001; accepted October 15, 2001.

Reprint requests: Irene Georgakoudi, PhD, MIT Spectroscopy Laboratory, 77 Massachusetts Ave, Rm 6-014, Cambridge, MA 02139. E-mail: ireneg@mit.edu

0002-9378/2002 $35.00 + 0 ***6/1/121075***

doi:10.1067/mob.2002.121075

Colposcopy and biopsy are the standard methods of diagnosing precancerous lesions in the uterine cervix. Although colposcopy is quite sensitive in detecting tissue abnormalities, it has very low specificity, even when performed by an experienced gynecologist.[1] As a result, a significant number of abnormal colposcopic examinations result in a normal biopsy, needlessly consuming health care resources. Techniques that provide a more precise assessment of underlying preinvasive disease could reduce the frequency of unnecessary biopsy and, potentially, permit a single-visit triage strategy that bypassed biopsy.

Spectroscopic modalities have been under development as a method for diagnosing disease for a number of years. Fluorescence spectroscopy has been studied extensively in several tissues. Its success as a technique for the detection of neoplastic changes is based on the hypothesis that the development of neoplasia is accompanied by modification in the biochemical composition of tissue. The latter can be assessed by the fluorescence spectral signatures of fluorescing biochemicals. Promising results have been acquired for several organs, demonstrating the potential of this technique as a clinical tool.[2,3] Several studies of in vivo fluorescence measurements of normal and precancerous cervical tissues indicate that spectroscopy could be a useful guide for the detection of cervical lesions during colposcopy.[4-8] Analysis of the

measured fluorescence is typically based on purely statistical rather than model-based quantitative methods. In the case of autofluorescence measurements, which are usually recorded in the 400 to 600 nm region, the spectra can be highly distorted by tissue scattering and absorption. Elimination of these artifacts and recovery of the intrinsic (undistorted) tissue fluorescence is not trivial. Knowledge of scattering and absorption is required for each patient and each site examined because these properties can vary considerably.

Other spectroscopic techniques, such as diffuse reflectance and light-scattering spectroscopy (LSS), have also shown promise as diagnostic tools. Diffuse reflectance spectroscopy (DRS) provides information on the absorption and reduced scattering coefficients of tissue.[9] Differences in these tissue properties between normal and high-grade squamous intraepithelial lesions (SILs) have been reported in the uterine cervix.[10]

LSS is a novel technique that provides morphologic information about the number and size distribution of nuclei of the epithelial cell layer.[11] Its potential as a diagnostic tool has been demonstrated for a number of tissues (such as Barrett's esophagus, the bladder, the oral cavity, and the colon).[12] Changes in nuclear morphologic features are well-established histopathologic hallmarks of precancerous and cancerous changes. LSS allows us to study such changes in vivo without the need for tissue excision and processing.

In this preliminary study, we evaluated the potential of 3 in vivo spectroscopic techniques (intrinsic fluorescence spectroscopy [IFS], DRS, and LSS) individually and in combination (trimodal spectroscopy [TMS]) as tools for the biochemical and morphologic characterization of normal squamous epithelium, squamous metaplastic epithelium, and SILs of the uterine cervix. Specifically, we illustrate how IFS can be used to extract diagnostically useful quantitative information about the biochemical composition of cervical tissue and the changes that take place during the development of premalignancies. We use DRS to assess changes in the scattering and absorption properties between normal and neoplastic tissues. We report the first results of in vivo LSS studies of cervical tissue and demonstrate that this technique can be used to extract important diagnostic information about the nuclear size distribution of cervical tissue. Finally, because each one of the techniques provides complementary information about tissue biochemistry and morphologic condition, we combine them to assess the diagnostic potential of TMS compared with each one of the techniques alone.

Methods

Data were collected from 44 patients who underwent colposcopy after an abnormal Papanicolaou smear. The cervix was examined under colposcopic vision at 15× magnification. After application of 3% acetic acid to the cervix, spectra were acquired from 1 or 2 colposcopically normal ectocervical sites located outside of the transformation zone and any colposcopically abnormal sites. Immediately after spectral acquisition, the suspicious sites were biopsied. The biopsy specimens were examined and classified by an experienced pathologist, and the classification was correlated with the results of spectroscopy. This preliminary study was designed as a companion study to standard colposcopy and biopsy procedures. For this reason, the acquisition of additional biopsy specimens of colposcopically normal tissue could not be justified. Thus, we examined spectroscopically only colposcopically normal tissues away from the transformation zone, where the chances of underlying metaplasia or a lesion are minimal. Reflectance and fluorescence spectra were collected from 50 colposcopically normal squamous ectocervical (NSE) tissue sites that were not biopsied, 5 biopsied sites that were classified histopathologically as benign or mature squamous epithelium (MSE), 16 biopsied sites that were classified as squamous metaplasia (SQM), and 13 biopsied sites that were classified as SIL, 2 of which sites were low-grade SILs and the remaining 11 were high-grade SILs. The biopsied MSE and SQM sites are referred to collectively as biopsied non-SILs. This study was approved by the Institutional Review Board at the Brigham and Women's Hospital, where this study was conducted, and the Massachusetts Institute of Technology's Committee On the Use of Humans as Experimental Subjects.

A fast excitation-emission matrix (EEM) instrument, described in detail previously,[13] was used for recording cervical tissue fluorescence and reflectance spectra in vivo. The fast EEM provides several laser excitation wavelengths, each one of which leads to the emission of a distinct fluorescence emission spectrum. Thus, we can consider variations in fluorescence intensity at a particular emission wavelength as a function of the excitation wavelength (excitation spectrum) and over a range of emission wavelengths at a specific excitation wavelength (emission spectrum); hence, the name EEM. Light was delivered and collected from the tissue with an optical fiber probe, which was brought in gentle contact with the tissue. The excitation light was of low energy and did not damage the tissue. Fluorescence spectra at 11 excitation wavelengths between 337 and 610 nm and a white light (350-700 nm) reflectance spectrum were acquired in less than 1 second. The measurement was repeated 3 times; the probe was removed, and if the site appeared colposcopically abnormal, it was biopsied. The intraclinician variation (ie, the variation in the intensity of the measured spectra, when the same tissue site was examined by the same clinician multiple times) was approximately 5%. A temporary mark left on the tissue by contact with the probe sheath was used to ensure that the biopsied site was the same as the site from which

spectra were recorded. The measured fluorescence and reflectance spectra were analyzed to provide 3 types of spectroscopic information: intrinsic fluorescence, diffuse reflectance, and light scattering.

Intrinsic fluorescence spectroscopy. To extract the intrinsic tissue fluorescence, fluorescence and reflectance spectra acquired within 1 second were combined with the use of a photon migration model.[14] This model is based on the fact that fluorescent and reflected photons undergo similar scattering and absorption events as they traverse the tissue. Thus, information from the distortions that are introduced in tissue reflectance spectra by scattering and absorption can be used to remove such distortions from the measured tissue fluorescence spectra.

In contrast with measured fluorescence spectra, which consist of a nonlinear combination of fluorescence, scattering, and absorption information, the resulting intrinsic fluorescence EEMs could be described by a linear combination of collagen and NAD(P)H (the reduced form of nicotinamide adenine dinucleotide) EEMs with the use of least-squares fitting. Thus, quantitative information on the biochemical composition of tissue was extracted in vivo. Collagen and NAD(P)H are the main tissue fluorophores in the visible region of the spectrum.[15] NAD(P)H is found mainly in the epithelial cell layer and is sensitive to the metabolic activity and the redox state of tissue.[16] Collagen is a major component of the extracellular matrix and dominates the stromal fluorescence. Because fluorescence is sensitive to the local environment of the chromophore, it was essential for the quantitative analysis of tissue intrinsic fluorescence to determine the collagen and NAD(P)H EEMs in an in vivo environment.[17]

Diffuse reflectance spectroscopy. Diffuse reflectance spectra were analyzed with a model that is based on the light-diffusion theory to extract the absorption and reduced scattering coefficients of cervical tissue.[9] Hemoglobin, which is present only in the stroma, is considered to be the main tissue absorber in the visible range of the spectrum. The scattering properties of diffusely reflected light are affected mainly by the collagen fibers of the stroma. Thus, DRS provides information primarily on the morphologic condition and biochemistry of the stroma.

Light-scattering spectroscopy. A small fraction (2%-5%) of the back-reflected light is due to photons that are singly back-scattered by the cell nuclei of the epithelium.[11] This LSS spectrum is extracted from the reflectance data by subtracting the diffuse component that was provided by the model of Zonios et al.[9] The intensity of the LSS spectrum varies in wavelength in an oscillatory manner. The frequency and depth of these oscillations depend on the size and number density of the scatterers (cell nuclei). These variations were analyzed with a model based on the theory of light scattering to determine the number and size of the epithelial cell nuclei.[11]

Trimodal spectroscopy. Because intrinsic fluorescence, diffuse reflectance, and light-scattering spectra were collected simultaneously from all tissue sites that were examined, we combined the information that was extracted from each one of the techniques to determine whether any improvements could be achieved in the diagnostic performance of these methods. Each one of the spectroscopically examined sites was assigned a classification as SIL or non-SIL that was consistent with at least 2 of the 3 spectroscopic techniques. The sensitivity and specificity of TMS (ie, the combined use of IFS, DRS and LSS) was then determined by a comparison of the spectroscopic and histopathologic classifications.

Statistical analysis. Logistic regression and "leave-1-out" cross-validation were used to determine and validate the diagnostic potential of the quantitative parameters that were extracted from the analysis of IFS, DRS, and LSS spectra.

In the case of IFS, 2 logistic regression decision lines were calculated on the basis of the relative NAD(P)H and collagen fluorescence contributions to the overall intrinsic tissue fluorescence. First, a decision line was calculated to separate the colposcopically NSE sites from the colposcopically abnormal sites, which reside typically in the transformation zone. Then, a second decision line was calculated to determine which of the transformation zone sites were SILs. To evaluate the sensitivity and specificity of this technique to separate SILs from non-SILs in an unbiased manner, we used "leave-1-out" cross-validation.[18] Specifically, the data from a particular site were eliminated, and logistic regression was used to form a decision line that classified the remaining sites in a manner that optimized agreement with the histopathologic classification. The resulting decision line was then used to classify the excluded site. This process was successively applied to each of the sites. Sensitivity and specificity values were determined by a comparison of the spectroscopic classification with that of histopathology. Statistical analysis was performed with the use of Matlab statistics software (The Math Works, Inc, Natick, Mass).

Logistic regression and "leave-1-out" cross-validation were also used to determine the sensitivity and specificity with which DRS and LSS parameters can characterize SILs and non-SILs when compared with the histopathologic evaluation. The slope and intercept of a line that described the wavelength dependence of the reduced scattering coefficient were used as the diagnostic parameters in the case of DRS; the number density and size SD of epithelial cell nuclei were used for LSS.

Results. Mean measured and extracted intrinsic fluorescence spectra for NSE, SQM, and SIL sites at 337 nm excitation are shown in Fig 1, *A* and *B*. Note the difference in line shape between the measured and intrinsic fluorescence, especially in the 420 nm region of the spectrum, where hemoglobin distortions are prominent. In

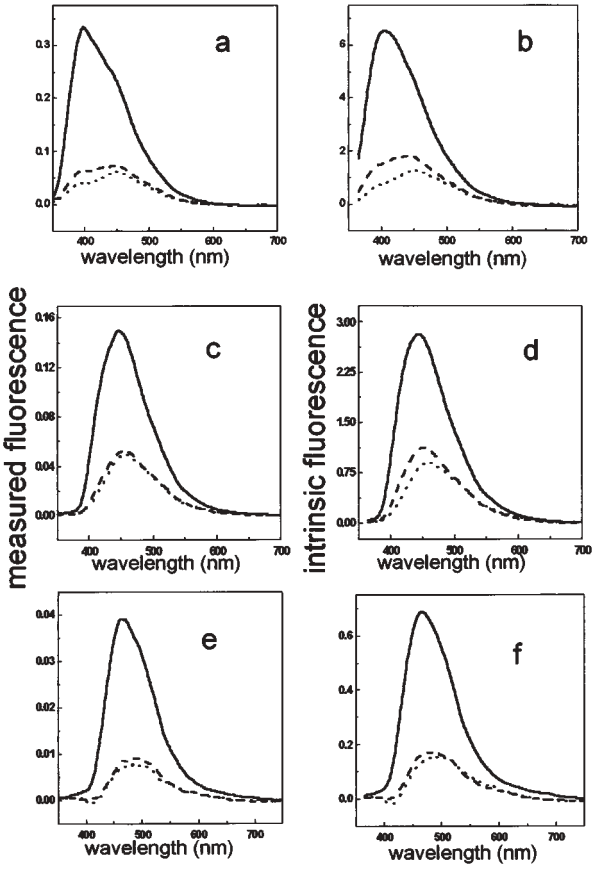

Fig 1. Mean measured fluorescence spectra for colposcopically normal (*solid line*), squamous metaplastic (*dashed line*), and SIL (*dotted line*) sites for excitation at 337 nm (**A**), 358 nm (**C**), and 397 nm (**E**). The corresponding mean intrinsic fluorescence spectra are shown in panels **B**, **D**, and **F** for 337, 358, and 397 nm excitation, respectively. The intensity of all measured fluorescence spectra (panels **A**, **C**, and **E**) and all intrinsic fluorescence spectra (panels **B**, **D**, and **F**) are plotted with the use of the same arbitrary unit scale.

addition, significant changes in the line shape and the intensity are observed between the intrinsic fluorescence of the sites inside (SQM and SIL) and outside (NSE) the transformation zone. Specifically, the intensity of the SQM and SIL sites decreases, and their line shape is broader and shifted to the red region of the spectrum, when compared with that of the NSE sites. Significant variations in fluorescence intensity are detected from patient to patient. However, differences between the NSE and SIL sites remain significant even when the SDs associated with the corresponding mean spectra are taken into account. A change in the line shape and the intensity between the mean SQM and SIL sites is also detected at 337 nm excitation. These differences are more pronounced in the intrinsic rather than in the measured fluorescence spectra (Fig 1, *A* and *B*).

At longer excitation wavelengths, the differences between measured and corresponding intrinsic fluorescence spectra become less pronounced (Fig 1, *C-F*). A substantial decrease in the intensity of the intrinsic fluorescence of SQM and SIL sites compared with that of NSE sites persists. However, the fluorescence line shapes of all 3 tissue types become very similar. Furthermore, the small intensity difference between the SQM and SIL sites that are observed at 337 nm excitation gradually decreases with longer excitation wavelengths.

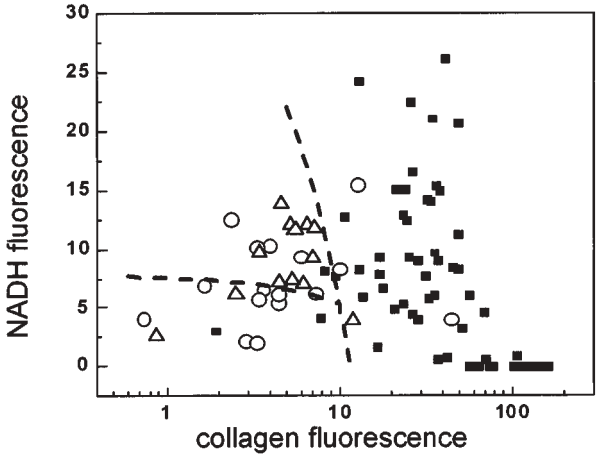

Fig 2. Collagen and NAD(P)H contributions to the overall intrinsic fluorescence for normal (*filled squares*), squamous metaplastic (*open circles*), and SIL (*open triangles*) sites. The decision lines are drawn on the basis of logistic regression analysis of the entire data set and are designed to separate colposcopically normal and abnormal sites (*vertical line*) and colposcopically abnormal non-SILs from SILs (*horizontal line*). The lines are not straight because the collagen fluorescence is plotted as a log scale to facilitate visualization of the entire data set.

A linear combination of NAD(P)H and collagen EEMs was sufficient to describe accurately the extracted cervical tissue intrinsic fluorescence spectra. The relative contributions of collagen and NAD(P)H fluorescence to the bulk tissue intrinsic fluorescence spectra are displayed in Fig 2 for NSE, SQM, and SIL sites. A significant decrease in the collagen contribution is observed for the SQM and SIL sites compared with the NSE sites. In addition, the NAD(P)H content of SILs is substantially higher than that of the SQMs. These features were exploited in a 2-step logistic regression and "leave-1-out" cross-validation analysis performed to separate initially the NSE and MSE sites from the biopsied SQMs and SILs of the transformation zone and then the SILs from the SQMs. The logistic regression lines that optimize the agreement between the histopathologic and spectroscopic classification are included in Fig 2. To validate the results of logistic regression, "leave-1-out" cross-validation was used. The sensitivity and specificity that are achieved in this manner for separating the biopsied SILs from the biopsied non-SILs (MSEs and SQMs) and the biopsied SILs from all spectroscopically examined non-SILs (NSEs, MSEs and SQMs) are shown in the Table.

Table. Performance of different spectroscopic techniques for separating SILs from non-SILs

	Biopsied non-SILs vs SILs (%)*		*Non-SILs† vs SILs (%)*	
Technique	*Sensitivity*	*Specificity*	*Sensitivity*	*Specificity*
IFS	62	67	62	92
DRS	69	57	62	82
LSS	77	71	77	83
TMS	92	71	92	90

*Biopsied non-SILs include 21 colposcopically abnormal biopsied sites that were classified as MSE (5/21 sites) or SQM (16/21 sites).
†Non-SILs in this case include 50 colposcopically normal sites and 21 biopsied sites that were classified as SQM or MSE.

Mean reflectance spectra for the NSE, SQM, and SIL sites are shown in Fig 3, *A*. The prominent decrease in intensity at approximately 420 nm is due to hemoglobin absorption. Small changes in the overall intensity and line shape of the mean spectra for each tissue type are observed. However, there are significant interpatient variations.

Diffuse reflectance spectra were analyzed with a light diffusion theory–based model that was appropriate for the light/delivery collection geometry of the fast EEM.[9] Examples of reflectance spectra measured from an SQM and a high-grade SIL site with the corresponding model fits are shown in Fig 3, *B*. The observed reflectance spectra are described well by the model. The reduced scattering coefficients (μ_s') as a function of wavelength, λ, that were extracted from the diffuse reflectance analysis, are shown in Fig 3, *C*, for the 2 sites. To characterize the overall intensity and slope of these spectra, a linear fit was performed to $\mu_s'(\lambda)$. The intercepts at λ, = 0 nm and the slopes of the fitted lines for all sites are shown in Fig 3, *D*. A trend towards smaller and flatter $\mu_s'(\lambda)$ is observed, particularly between the NSE and MSE sites and the biopsied SQMs and SILs. Logistic regression and "leave-1-out" cross-validation were performed to determine the diagnostic potential of this technique as in the case of IFS. The corresponding sensitivity and specificity values are included in the Table.

To extract the light-scattering spectrum that corresponds to a particular site, the modeled diffusely reflected light component was subtracted from the measured reflectance spectrum. The corresponding LSS spectra for the SQM and SIL reflectance spectra of Fig 3, *B*, are depicted in Fig 4, *A*. These spectra were analyzed with the use of a model that is based on the theory of light scattering to extract the size distribution of the scattering particles, which in this case are nuclei of the epithelial cell layer.[11,12] The nuclear size distributions of the 2 representative sites are shown in Fig 4, *B*. We note that the SD of the SIL nuclear size distribution is larger than that of the SQM site. In addition, the total number of nuclei per unit area is larger for the SIL than for the SQM site.

The nuclear number density as a function of the SD of nuclear size is shown in Fig 4, *C*. Logistic regression and cross-validation were performed to determine the sensitivity and specificity with which the LSS parameters can distinguish SILs from non-SILs (Table). This technique exhibits the highest sensitivity of the 3 spectroscopic techniques that were examined.

When information from all 3 spectroscopic techniques are combined to classify a particular site (TMS), the sensitivity and specificity with which SILs can be distinguished from non-SILs increases significantly (Table).

Comment

In this report, we demonstrate how 3 different spectroscopic techniques (intrinsic fluorescence, diffuse reflectance, and light scattering) can be used to extract noninvasively quantitative biochemical and morphologic information pertaining to a particular tissue site. The focus of this study has been the spectroscopic evaluation of normal, squamous metaplastic (benign), and precancerous (SILs) sites of the uterine cervix. This work demonstrates that spectroscopic signatures that are characteristic of each 1 of these tissue types can be extracted and used by a clinician as a means of improving the current methods for diagnosing SILs after a positive screening test.

In contrast with previous fluorescence spectroscopy studies, which relied on statistical diagnostic algorithms, we used IFS to extract quantitative tissue biochemical information. The intrinsic fluorescence spectra of cervical tissue could be described by a linear combination of the spectra of 2 biochemical components, NAD(P)H and collagen.

This biochemical decomposition indicates that the collagen content of the colposcopically abnormal sites is significantly lower than that of the colposcopically normal sites. Significant decreases in cervical collagen autofluorescence have also been detected in Charles-Dawley rats in vivo during gestation.[19] It is possible that the detected decrease in collagen fluorescence is the result of a reduced number of collagen cross-links within the colposcopically abnormal tissue sites, typically found in the transformation zone. It has been shown that collagenases, enzymes responsible for the degradation of collagen cross-links, are usually present in tissue areas undergoing significant architectural changes, as in the case of wound healing and tissue regeneration.[20] Because

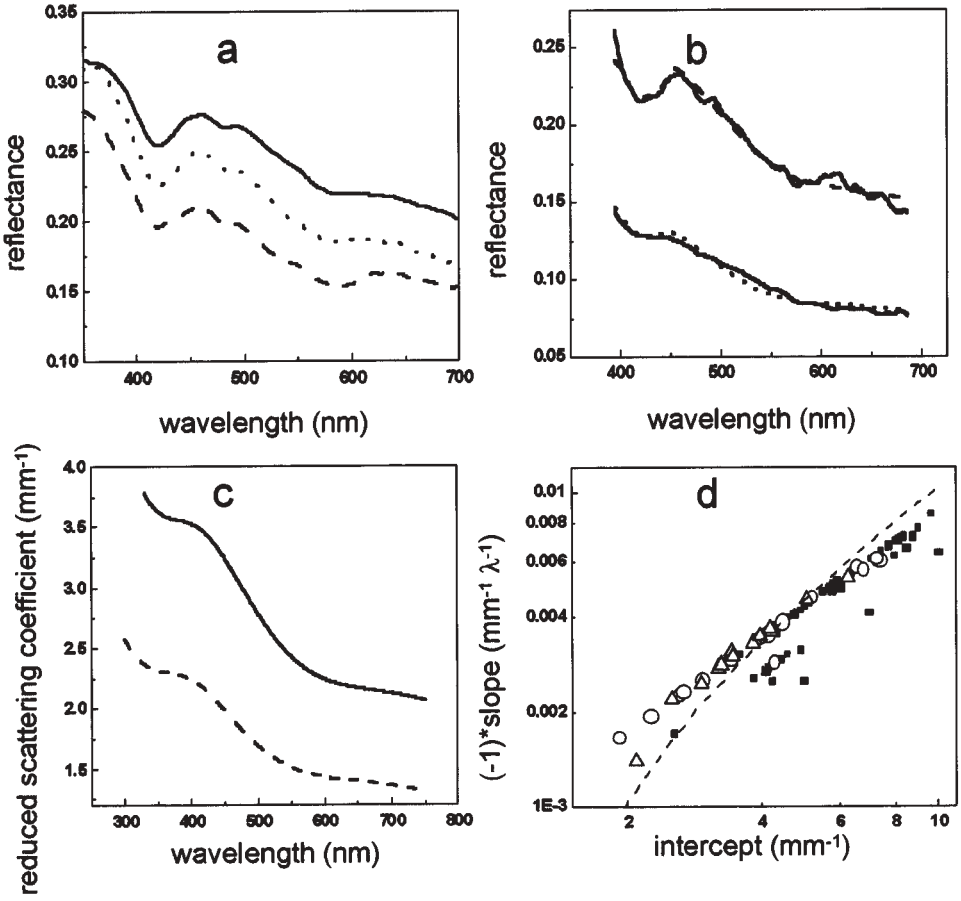

Fig 3. A, Mean reflectance spectra for colposcopically normal (*solid line*), squamous metaplastic (*dashed line*), and SIL (*dotted line*) sites. **B**, Measured reflectance spectra (*solid lines*) and corresponding fits (*dashed and dotted lines*) were achieved with the use of a light diffusion–based model. Upper spectrum: squamous metaplastic site; lower spectrum: high-grade SIL. **C**, Reduced scattering coefficients that were extracted from the diffuse reflectance analysis of the squamous metaplastic (*solid line*) and high-grade SIL (*dashed line*) reflectance spectra that are shown in **B**. **D**, Slope and intercept of the wavelength-dependent reduced scattering coefficient that was extracted from the analysis of the diffuse reflectance spectra for normal (*filled squares*), squamous metaplastic (*open circles*), and SIL (*open triangles*) sites were used in the diagnostic algorithm. The *dashed line* represents the logistic regression decision line that separates SILs from non-SILs.

the transformation zone of the uterine cervix is an area undergoing constant change, it is possible that the reduction in collagen fluorescence is the result of an increase in the expression of collagenases. In addition, it has been reported recently that small differences can be found in the levels and/or patterns of expression of matrix metalloproteinases, a family of collagenases, in normal squamous epithelium, squamous metaplastic, and SIL sites of the uterine cervix.[21] In addition, the observed fluorescence intensity decrease could be the result of an increase in epithelial thickness of the colposcopically abnormal sites, because in that case a smaller amount of light would be able to reach the stromal tissue layer, where collagen is found.

Although changes in the collagen contribution to the overall intrinsic tissue fluorescence spectra differentiate colposcopically normal from abnormal sites, a substantial difference in the NAD(P)H contribution is found for SILs when compared with the biopsied non-SIL sites. This increase could represent an increase in the thickness of the epithelium, or it could reflect an increase in the metabolic activity of the SILs.

The specific collagen and NAD(P)H contributions to the overall intrinsic tissue fluorescence can be used to develop diagnostic algorithms that are designed to distinguish SILs from non-SILs. Thus, quantitative biochemical tissue characterization provides insights in the specific biochemical changes that take place during the development of precancerous lesions, which in turn are useful diagnostically. Elegant and extensive in vivo fluorescence spectroscopic studies of cervical neoplasia have been performed by Ramanujam et al[4-7] and Mitchell et al.[8] Results have been published for data acquired from 95 patients and a total of 381 cervical sites at 3 different excitation wavelengths (337, 380 and 460 nm). Differences in the measured fluorescence spectra of normal, benign (in-

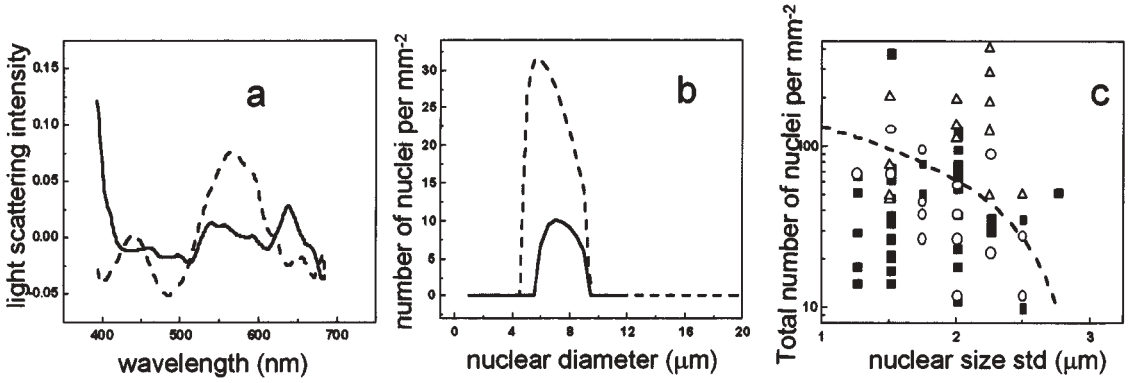

Fig 4. A, Light scattering spectra extracted after the subtraction of the diffuse reflectance component from the measured reflectance for the squamous metaplastic (*solid line*) and high-grade SIL (*dashed line*) sites that are shown in Fig 3, *B*. **B**, Nuclear size distributions extracted from the analysis of the squamous metaplastic and high-grade SIL LSS spectra that are shown in **A**. **C**, The number density of nuclei of the epithelial cell layer as a function of the SD of the corresponding nuclear size distribution for normal (*filled squares*), squamous metaplastic (*open circles*), and SIL (*open triangles*) sites. The decision line (*dashed line*) is drawn on the basis of the logistic regression analysis.

flammation / metaplasia), low-grade, and high-grade lesions were exploited with the use of principal component analysis. On the basis of this analysis, diagnostic algorithms were developed that distinguished SILs from non-SILs with a sensitivity of 82% and a specificity of 68% and distinguished high-grade SILs from non–high-grade SILs with sensitivity and specificity of 79% and 78%, respectively.[5] Our diagnostic algorithms were based on quantitative biochemical information that was extracted from intrinsic fluorescence EEMs that were acquired between 337 and 425 nm. Even though spectra were acquired at longer excitation wavelengths, they were not used for biochemical decomposition because we did not have available fluorescence EEMs of chromophores (such as flavin adenine dinucleotide), which could contribute to the acquired spectroscopic signals. Compared with the diagnostic performance of the biochemical decomposition performed with our intrinsic fluorescence spectra (sensitivity, 62%; specificity, 92%), the statistically based algorithm presented by Ramanujam et al[5] is more sensitive but less specific. Spectroscopic information acquired at 460 nm excitation, which was not used in our study, might contribute to the higher sensitivity reported in that study. We should also note that our experimental data set is smaller and consists of only 2 low-grade lesions.

Autofluorescence studies that were performed at 442 nm excitation with 3 patients reported an increase in red fluorescence between normal and malignant cervical tissue sites.[22] This increase was tentatively attributed to porphyrins. Porphyrin fluorescence was not detected in this and other studies that examined normal and cervical SILs.[23] However, it is possible that changes in the porphyrin content of cervical tissue take place when premalignant lesions progress to malignancy.

Changes are also observed in the scattering properties of SIL and non-SIL tissue sites, as determined by the analysis of the diffuse reflectance spectra. The scattering properties of the bulk tissue measured with our system are affected mainly by the collagen network of the stroma.[24] Thus, the observed decrease in the reduced scattering coefficient of SILs could be the result of changes in the density of the collagen network. However, it should be noted that an increase in the thickness of the epithelial layer could also be at least partly responsible for this decrease. Our results are consistent with a previous study that used near-infrared spectroscopy, which reported a 15% decrease in the effective scattering coefficient of high-grade SILs when compared with NSE.[10]

In vivo LSS measurements in cervical tissue are reported here for the first time. This technique provides detailed information on the number density and size distribution of epithelial cell nuclei.[11] In previous studies, we found that number density and nuclear enlargement (percentage of cell nuclei larger than 10 μm in diameter) were the most diagnostically significant parameters that were extracted.[12] In the case of cervical tissue, we observed that the SD of the nuclear size distribution is a better diagnostic parameter than nuclear enlargement.

The nuclear morphometric parameters extracted from the LSS measurements can be used to develop algorithms for distinguishing SILs from non-SILs. LSS provides the most sensitive diagnosis, while maintaining high levels of specificity (ie, small number of false-positive results). Nonetheless, these results should be considered preliminary, given the relatively small sample size.

In the final step of our analysis, we combined the results of all 3 spectroscopic techniques to make a consensus diagnosis on the classification of a particular site. We find that the sensitivity and specificity of separating SILs from non-SILs are enhanced significantly as compared with the results of each one of the techniques used individually. This enhancement is expected, because each 1 of the spec-

troscopic techniques provides complementary information. A similar enhancement has been observed with the application of TMS for detecting dysplasia in Barrett's esophagus.[25] Note that for this data set, the use of TMS would eliminate 71% of nondiagnostic biopsy results.

The significantly higher specificity achieved with TMS demonstrates that it can serve as a useful guide for the physician to biopsy sites that are lesions and to avoid the biopsy of sites that are colposcopically abnormal but are not neoplastic. These results compare favorably with the sensitivity and specificity of colposcopic impression for distinguishing SILs from non-SILs.[1] Analysis of extensive studies on the performance of repeated colposcopy visits indicate that, although the sensitivity of colposcopy is generally very high (≤94%), its specificity is significantly lower (≤51%) and highly variable.

Even though we achieve a significant improvement in sensitivity and specificity when we combine information from all 3 spectroscopic techniques, agreement between spectroscopic and histopathologic evaluation is not perfect. Sampling or misregistration errors (ie, spectral acquisition from a tissue site that is slightly different from the biopsied site) could obviously result in different classifications. We are in the process of modifying our probes to eliminate any such errors. In addition, it is possible that for the spectroscopically false-positive sites, the presence of disease was not detected histopathologically because only a limited portion of the biopsied tissue was examined under the microscope. We are developing a protocol that involves extensive serial sectioning of biopsied tissue to address this issue.

In summary, this study assessed the potential of a novel method, TMS, as a tool for the sensitive and specific detection of squamous lesions in the uterine cervix. The 3 techniques (intrinsic fluorescence, diffuse reflectance and light scattering) are implemented simultaneously and provide information about different aspects of tissue biochemistry and morphology that are altered during the development of cervical SILs. In addition to its excellent diagnostic potential, TMS is a rich source of quantitative information that improves our understanding of the changes that take place during neoplastic transformation. Our results demonstrate that TMS could be used to guide the selection of biopsy sites during colposcopy. To achieve this goal, we are in the process of developing software that allows data analysis in real time. Real time data analysis will also allow us to determine more accurately the sensitivity and specificity of TMS in a prospective manner. Ultimately, our aim is to extend these measurements to an imaging modality that would allow the entire cervix to be spectroscopically examined and the progression or regression of a specific lesion site to be identified.

We thank Dr Jacques Van Dam for his support and enthusiasm, which were crucial during the conception and early stages of this project, and Noreen Fitzgerald for assistance with patient recruitment.

REFERENCES

1. Mitchell MF. Accuracy of colposcopy. Consult Obstet Gynecol 1994;6:70-3.
2. Wagnières GM, Star WM, Wilson BC. In vivo fluorescence spectroscopy and imaging for oncological applications. Photochem Photobiol 1998;68:603-32.
3. Ramanujam N. Fluorescence spectroscopy of neoplastic and non-neoplastic tissues. Neoplasia 2000;2:89-117.
4. Ramanujam N, Mitchell M, Mahadevan A, et al. In vivo diagnosis of cervical intraepithelial neoplasia using 337-nm-excited laser-induced fluorescence. Proc Natl Acad Sci 1994;91:10193-7.
5. Ramanujam N, Follen-Mitchell M, Mahadevan-Jansen A, et al. Cervical precancer detection using a multivariate statistical algorithm based on laser-induced fluorescence spectra at multiple excitation wavelengths. Photochem Photobiol 1996;64:720-35.
6. Ramanujam N, Follen-Mitchell M, Mahadevan-Jansen A, et al. Spectroscopic diagnosis of cervical intraepithelial neoplasia (CIN) in vivo using laser-induced fluorescence spectra at multiple excitation wavelengths. Lasers Surg Med 1996;19:63-74.
7. Ramanujam N, Follen-Mitchell M, Mahadevan A, et al. Development of a multivariate statistical algorithm to analyze human cervical tissue fluorescence spectra acquired in vivo. Lasers Surg Med 1996;19:46-62.
8. Mitchell M, Cantor S, Ramanujam N, Tortolero-Luna G, Richards-Kortum R. Fluorescence spectroscopy for diagnosis of squamous intraepithelial lesions of the cervix. Obstet Gynecol 1999;93:462-70.
9. Zonios G, Perelman LT, Backman V, et al. Diffuse reflectance spectroscopy of human adenomatous colon polyps in vivo. Appl Optics 1999;38:6628-37.
10. Hornung R, Pham T, Keefe K, Berns M, Tadir Y, Tromberg B. Quantitative near-infrared spectroscopy of cervical dysplasia in vivo. Hum Reprod 1999;14:2908-16.
11. Perelman L, Backman V, Wallace M, et al. Observation of periodic fine structure in reflectance from biological tissue: a new technique for measuring nuclear size distribution. Phys Rev Lett 1998;80:627-30.
12. Backman V, Wallace M, Perelman L, et al. Detection of preinvasive cancer cells. Nature 2000;406:35-6.
13. Zângaro RA, Silveira L, Manoharan R, et al. Rapid multiexcitation fluorescence spectroscopy system for in vivo tissue diagnosis. Appl Optics 1996; 35:5211-9.
14. Zhang Q, Müller MG, Wu J, Feld MS. Turbidity-free fluorescence spectroscopy of biological tissue. Optics Lett 2000;25:1451-3.
15. Richards-Kortum R, Sevick-Muraca E. Quantitative optical spectroscopy for tissue diagnosis. Annu Rev Phys Chem 1996; 47:555-606.
16. Mayevsky A, Chance B. Intracellular oxidation-reduction state measured in situ by a multichannel fiber-optic surface fluorometer. Science 1982;217:537-40.
17. Georgakoudi I, Jacobson BC, Müller MG, et al. NAD(P)H and collagen as in vivo quantitative fluorescent biomarkers of epithelial pre-cancerous changes. Cancer Res. In press.
18. Schumacher M, Hollander N, Sauerbrei W. Resampling and cross-validation techniques: A tool to reduce bias caused by model building? Stat Med 1997;16:2813-27.
19. Glassman W, Byam-Smith M, Garfield R. Changes in rat cervical collagen during gestation and after antiprogesterone treatment as measured in vivo with light-induced autofluorescence. Am J Obstet Gynecol 1995;173:1550-6.
20. Ellis DL, Yannas IV. Recent advances in tissue synthesis in vivo by use of collagen-glycosaminoglycan copolymers. Biomaterials 1996;17:291-9.
21. Talvensaari A, Apaja-Sarkkiner M, Hoyhtya M, Westerlund A, Puistola U, Tuppeernniemi-Hujanen T. Matrix metalloproteinase 2 immunoreactive protein appears early in cervical epithelium dedifferentiation. Gynecol Oncol 1999;72:306-11.

22. Koumantakis E, Vasileiou A, Makrigiannakis A, Unsöld E, Papazoglou T. Spectral variations of laser-induced tissue emission during in vivo detection of malignancies in the female genital tract. J Photochem Photobiol B: Biol 1997;40:183-6.
23. Mahadevan A, Follen-Mitchell M, Silva E, Thomsen S, Richards-Kortum R. Study of the fluorescence properties of normal and neoplastic human cervical tissue. Lasers Surg Med 1993;13:647-55.
24. Saidi I, Jacques S, Tittel F. Mie and Rayleigh modeling of visible-light scattering in neonatal skin. Appl Optics 1995;34: 7410-8.
25. Georgakoudi I, Jacobson B, Van Dam J, et al. Fluorescence, reflectance and light scattering spectroscopy for evaluating dysplasia in patients with Barrett's esophagus. Gastroenterology 2001;120:1620-9.